Desalination and Water Treatment
www.deswater.com

doi: 10.5004/dwt.2018.23099

132 (2018) 281–286
November

Effect of reactants molar ratio on photocatalytic activity of $(BiO)_2CO_3$ prepared by a hydrothermal routine

Jiufu Chen, Chaozhu Cheng, Junbo Zhong*, Jianzhang Li*

Key Laboratory of Green Catalysis of Higher Education Institutes of Sichuan, College of Chemistry and Environmental Engineering, Sichuan University of Science and Engineering, Zigong, 643000, China, email: cjf2171@163.com (J. Chen), 512563276@qq.com (C. Cheng), junbozhong@163.com (J. Zhong), lyl63@sina.com (J. Li)

Received 10 March 2018; Accepted 3 September 2018

ABSTRACT

In this work, a series of $(BiO)_2CO_3$ photocatalysts were successfully fabricated using a hydrothermal method by adjusting the molar ratio of $Bi(NO_3)_3{\cdot}5H_2O$ and urea (Bi/C). The results demonstrate that the molar ratio of $Bi(NO_3)_3{\cdot}5H_2O$ and urea (Bi/C) can significantly influence the samples obtained and the corresponding photocatalytic performance. When Bi/C is between 1/4 and 1/7, $(BiO)_2CO_3$ was successfully obtained. Furthermore, the molar ratio of Bi/C can affect the separation rate of photo-induced charge pairs, confirmed by results of surface photovoltage spectroscopy (SPS). The photocatalytic activities of the as-obtained samples were tested using methyl orange (MO) as a target pollutant. The results reveal that the sample prepared with 1/5 molar ratio of Bi/C exhibits the highest photocatalytic activity under simulated sunlight irradiation, which can be tightly attributed to its higher photo-generated carriers separation efficiency than other samples.

Keywords: Semiconductor; $(BiO)_2CO_3$; Photocatalytic performance; Hydrothermal method; Discoloration

1. Introduction

With the rapid development of industries and economy, environmental pollution caused by the organic pollutants has become a severe threat to the survival and development of human beings during the past few decades. Therefore, it is indispensable to re-mediate the environment by completely decomposing the organic pollutants. Nowadays, tremendous approaches, such as adsorption, biodegradation, membrane filtration technology and so on, have been exploited. However, all these methods have inherent shortages and cannot completely and effectively degrade all the organic pollutants. In view of the need of environment purification, it is urgent to develop new method for organic pollutants. As a promising pollutant degradation technology, semiconductor-based photocatalysis has been considered to be the most prospective way to eliminate contaminants due to its low-cost, environmental-friendly and no secondary pollution merits compared with the conventional decontamination methods [1–5].

Among the numerous semiconductor photocatalysts studied, $(BiO)_2CO_3$, as a typical sillén phase compound constructed by alternating $(Bi_2O_2)^{2+}$ layers and CO_3^{2-} layers, has received substantial research attentions recently due to its potential photocatalytic applications [6–9]. However, the wide band gap (2.87–3.58 eV) and high recombination rate of photo-generated carriers severely hinder its photocatalytic performance [10–13]. Up to now, tremendous investigations have been carried out to boost the photocatalytic performance of $(BiO)_2CO_3$, such as fabrication of $(BiO)_2CO_3$ with various morphologies, construction $(BiO)_2CO_3$-based heterostructures, nonmetal doping, noble-metal deposition and so on [14–20]. However, the relationship between the different reactant molar ratios and photocatalytic activity of $(BiO)_2CO_3$ prepared by a hydrothermal method has seldom addressed.

Herein, $(BiO)_2CO_3$ photocatalyst was prepared via a facile hydrothermal method using bismuth nitrate pentahydrate ($Bi(NO_3)_3{\cdot}5H_2O$) and urea as the initial reagents. Since

*Corresponding author.

the partially self-decomposition of urea during the reaction process can influence the formation as well as the photocatalytic performance of the final $(BiO)_2CO_3$ product [21], therefore it is necessary to investigate the effect of different molar ratios of reactant on the preparation and photocatalytic activity of $(BiO)_2CO_3$. The results indicate that the different reactant molar ratios can significantly affect the separation rate of photo-generated charge carriers, therefore influencing the corresponding photocatalytic performance of the as-synthesized $(BiO)_2CO_3$ accordingly.

2. Experimental section

2.1. Preparation of the samples

All the chemical reagents used in this work were of analytical grade and purchased from Chengdu Kelong Chemical Reagent Corporation without any further treatments. In a typical synthesis procedure, 0.02 mol bismuth nitrate pentahydrate ($Bi(NO_3)_3{\cdot}5H_2O$) was dissolved in 70 mL of dilute nitric acid (1+9) under intense stirring, then desired urea was added into above solution and the molar ratio of Bi/C was 1/1, 1/2, 1/3, 1/4, 1/5, 1/6 and 1/7 by controlling the amount of urea, respectively. After ultrasonic treatment for 10 min, the resulting mixture was then transferred into a 100 mL Teflon-lined stainless-steel autoclave and hydrothermally treated at 453 K for 24 h. When the autoclave was cooled down to room temperature naturally, the final product was collected by filtration, washed with deionized water and absolute ethanol repeatedly, and then dried in an oven at 333 K overnight for further use. The samples obtained with different Bi/C molar ratios (1/1, 1/2, 1/3, 1/4, 1/5, 1/6 and 1/7) were labeled as 1:1, 1:2, 1:3, 1:4, 1:5, 1:6 and 1:7, respectively.

2.2. Characterization of the samples

Crystallographic structures of the samples were obtained by X-ray diffraction (XRD) using a DX-2600 X-ray diffractometer at 40 kV and 25 mA with Cu-Kα (λ = 0.15406 nm) radiation. The scanning rate was kept at 0.05°/s and the scanning range from 10° to 70°. The UV-Vis diffuse reflectance spectra (DRS) of the samples were measured on a TU-1950 UV-Vis spectrophotometer using $BaSO_4$ as the reflectance standard. The specific surface area was determined over a SSA-4200 automatic surface analyzer based on Brunauer-Emmett-Teller (BET) equation. Scanning electron microscopy (SEM) images were taken on a VEGA 3SBU scanning electron microscope with an accelerating voltage of 15 kV. High-resolution transmission electron microscopy (HRTEM) was observed on a Tecnai TEM G2 microscope with an accelerating voltage of 300 kV. The measurements of surface photovoltage spectroscopy (SPS) were performed as the recipe given in the Ref. [22]. Nitrotetrazolium blue chloride (NBT) experiments were carried out following the procedures given in the Ref. [23].

2.3. Photocatalytic test

The photocatalytic activities of the as-prepared samples were evaluated on a Ph chem III photochemical reactor (Beijing NBET Technology Co., Ltd., China) by the discoloration of MO aqueous solution under simulated solar light irradiation. A 500 W Xeon lamp was served as the light source. In a typical experiment, 50 mg sample was added into a quartz tube containing 50 mL of 10 mg L^{-1} MO aqueous solution, the initial pH of MO was adjusted to 7.0, and then the suspension system was exposed to the light under intense magnetic stirring. After irradiation 40 min, the suspension was centrifuged to remove the photocatalyst powder. The degradation efficiency of MO was measured on a spectrophotometer using Lambert-Beer law. Trapping experiments for active free radicals were operated as the photocatalytic activity experiments mentioned above except for the existence of additional scavengers in the reaction system, the dosage of scavenger was 0.2 mmol·L^{-1} and the illumination time was 40 min.

3. Results and discussion

3.1. Characterization of the samples

When the molar ratio of Bi/C is 1/1, no solid samples were obtained. Fig. 1 shows the XRD patterns of the samples prepared. Seen from Fig.1, when the molar ratio of Bi/C is 1/2 and 1/3, no distinct peaks corresponding to $(BiO)_2CO_3$ were observed. The above results indicate that no $(BiO)_2CO_3$ can be generated under the low urea levels. However, it is interesting to note that when the molar ratio of Bi/C between 1/4 and 1/7, all the diffraction peaks of the samples can be readily indexed to the tetragonal $(BiO)_2CO_3$ (JCPDS No.41-1488), no impurity peaks or existence of other phases were detected, implying high purity of the samples. The XRD results indicate that the molar ratio of Bi/C can greatly influence the formation of $(BiO)_2CO_3$, which can be mainly ascribed to the partially self-decomposition of urea under high temperature [21]. In addition, the average crystallite size of (101) peak was estimated from the Scherrer equation. The average crystallite sizes of the 1:4, 1:5, 1:6 and 1:7 samples are 5.1 nm, 5.33 nm, 5.64 nm and 5.82 nm, respectively. These results suggest that the excessive urea can slightly promote grain growth of $(BiO)_2CO_3$, consequently increasing average crystallite sizes of the samples and changing the surface properties of the samples, such as

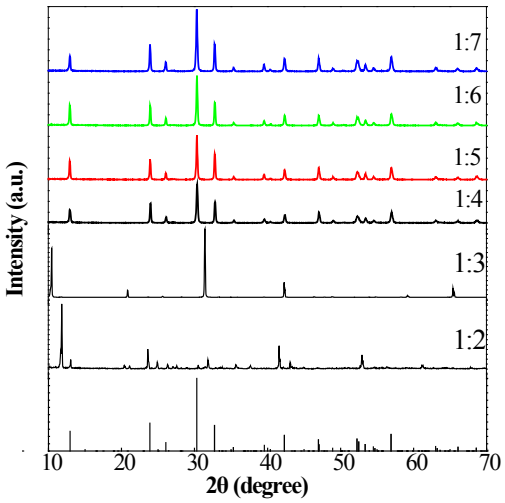

Fig. 1. XRD patterns of the photocatalysts.

the specific surface areas, the morphological microstructure and physical characteristics, which can be further proven by BET, SEM, SPS and NBT subsequently.

The specific area of the samples is displayed in Table.1. It shows that the specific surface areas of the 1:4, 1:5, 1:6 and 1:7 samples are 7.6, 9.7, 11.1 and 10.0 m^2/g, respectively. Considering the measurement error (± 5 m^2/g), these results confirm that the specific area of the as-prepared photocatalysts shows no distinct difference. Therefore, it demonstrates that molar ratio of Bi/C within a range cannot significantly affect the specific area parameter of $(BiO)_2CO_3$, thus the difference in photocatalytic performance is not caused by the specific area.

Table 1
Specific surface area of the photocatalysts

Photocatalyst	S_{BET} (m^2/g)
1:4	7.6
1:5	9.7
1:6	11.1
1:7	10.0

Scanning electron microscope (SEM) was used to further investigate the morphology and microstructure of the as-prepared photocatalysts. As displayed in Fig. 2, all the samples are composed of irregular sheet-like structure with no evident difference was observed, which manifests that different molar ratios of Bi/C cannot effectively influence the morphology of $(BiO)_2CO_3$. HRTEM is displayed in Fig. 2E, the spacing of 0.333 nm and 0.300 nm were clearly observed,which corresponds to (141) and (161) crystallographic planes of $(BiO)_2CO_3$, respectively. Combined with

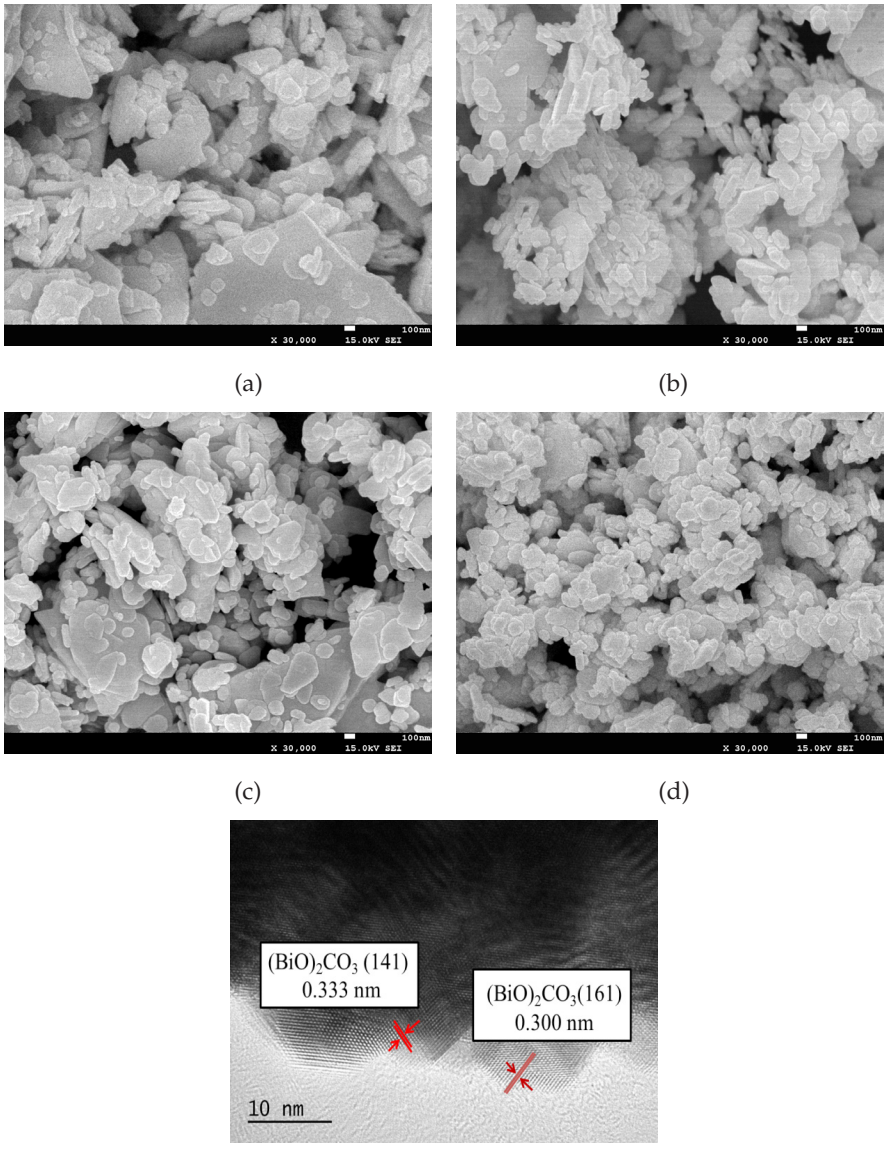

Fig. 2. SEM images of the photocatalysts; (A) 1:4; (B) 1:5; (C) 1:6; (D)1:7; (E) 1:5.

results of XRD, it is firmly apparent that the sample is $(BiO)_2CO_3$.

Fig. 3 displays the UV-Vis DRS of the 1:4, 1:5, 1:6 and 1:7 samples. As shown in Fig. 3, all the samples show similar UV-Vis DRS with the absorption edge at around 355 nm, and no evident red-shift or blue-shift was detected, demonstrating that different reactant molar ratios cannot alter the band gap of $(BiO)_2CO_3$. In addition, the band gap can be estimated by equation Eg = 1240/λ according to the Ref. [24], where Eg is the band gap (eV) and λ (nm) is the wavelength of the absorption edge in the spectrum. The calculated band gap of $(BiO)_2CO_3$ is about 3.49 eV, which agree well with the previous results [25,26].

SPS signal is an important parameter for photocatalyst, therefore it is essential to reveal the SPS properties of the samples. The SPS responses of $(BiO)_2CO_3$ synthesized with different molar ratios of Bi/C are exhibited in Fig. 4. All the as-prepared samples display distinct SPS responses in the ultraviolet wavelength range from 300–400 nm, which can be attributed to the intrinsic band gap absorption property of $(BiO)_2CO_3$. The SPS responses of the as-papered samples tend to increase as the urea content increasing, when the molar ratio of Bi/C is 1:5, the sample displays a much stronger SPS response as compared with other samples.

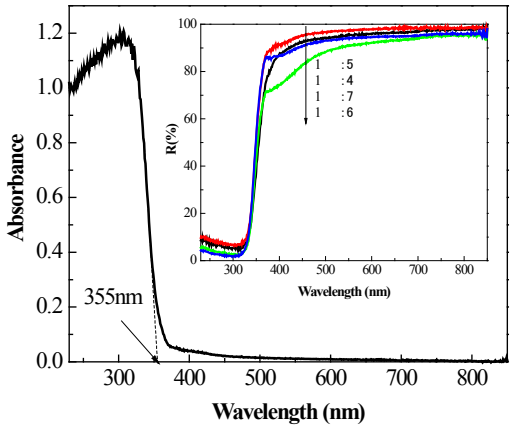

Fig. 3. UV-Vis diffuse reflectance spectra of the photocatalysts.

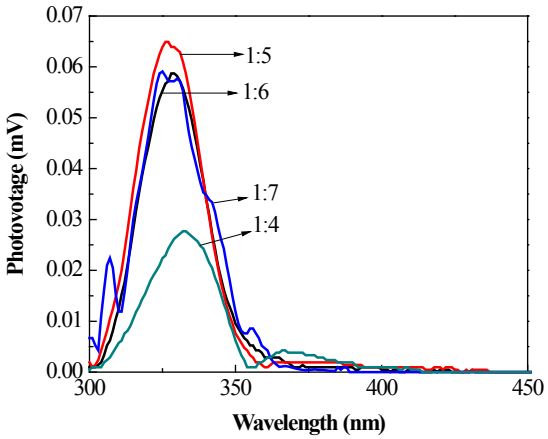

Fig. 4. SPS response of the photocatalysts.

According to the principle of SPS, a stronger SPS response corresponds to a higher separation rate of photo-generated carriers [27], thus the 1:5 sample possesses the highest charge separation efficiency, which is favorable to the photocatalytic performance. It is plausible that relative excessive urea can increase the content of oxygen vacancy in the surface of samples, so that the separation rate of photo-induced electron-hole pairs of $(BiO)_2CO_3$ can be enhanced. The results of SPS accord well with the results of photocatalytic activities.

In order to gain insight into the photocatalytic mechanism of $(BiO)_2CO_3$, the active free species in the photocatalytic process were detected. Isopropanol (IPA) [28,29], ammonium oxalate (AO) [30] and benzoquinone (BQ) [31] were used as scavengers to quench hydroxyl radicals (•OH), hole (h^+) and super oxide radicals ($•O_2^-$), respectively. As illustrated in Fig. 5, it is evident that the photocatalytic degradation efficiency of MO decreases only by 3.3% after adding IPA, demonstrating that •OH radicals play minor role in discoloration of MO. However, a distinct influence was observed after addition of AO and BQ with 26.1% and 64.3% reduction in the photocatalytic degradation efficiency of MO, respectively, which firmly indicates that $•O_2^-$ plays a dominant role while h^+ plays a secondary role in photocatalytic degradation of MO.

To further investigate the amount of $•O_2^-$ in the photoreaction system, NBT was used to detect the amount of $•O_2^-$ formed during the photocatalytic process. According to principle of NBT experiment, NBT can react with $•O_2^-$ to form insoluble purple formazan in the aqueous solutions, which will result in the decrease of NBT absorbance [32]. Namely, a lower absorbance of NBT solution suggests the existence of more $•O_2^-$ radicals in the photoreaction system, corresponding to a higher photo-generated carriers separation rate. Fig. 6 exhibits the NBT absorbance over the different photocatalysts, due to the partial overlap of the curves, only 1:4 and 1:5 samples were presented. Seen from Fig.6, the maximum absorbance of NBT over the 1:5 sample is lower than that over the 1:4 sample, indicating that 1:5 sample is more efficient in generating $•O_2^-$ radicals than the 1:4 sample, which implies that 1:5 sample possesses higher photo-generated carriers separation efficiency compared to the 1:4 sample. This result agrees well with the result of SPS,

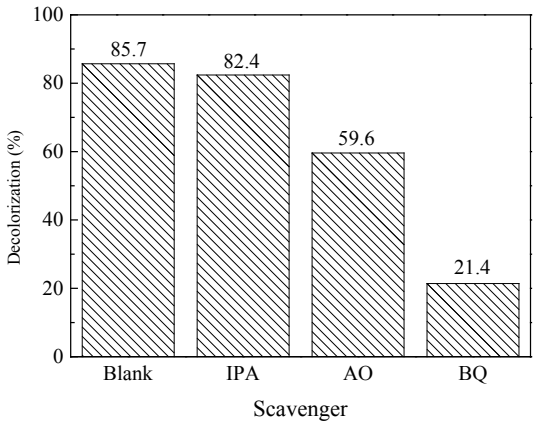

Fig. 5. The effects of a series of scavengers on the MO decolorization over the 1:5 sample.

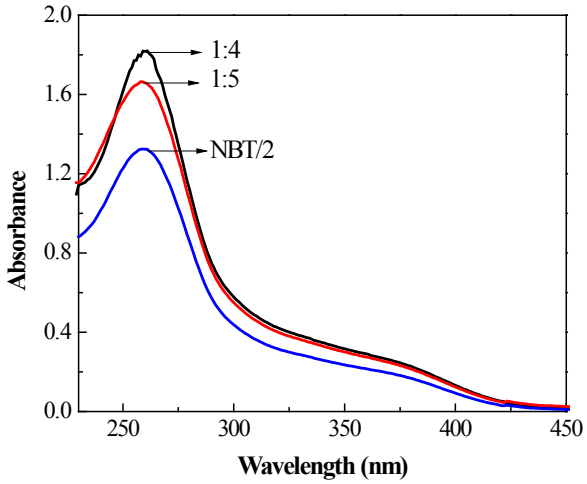

Fig. 6. Absorbance of NBT in the different photocatalytic system (illumination time = 20 min, NBT dosage = 0.05 mmol L^{-1}).

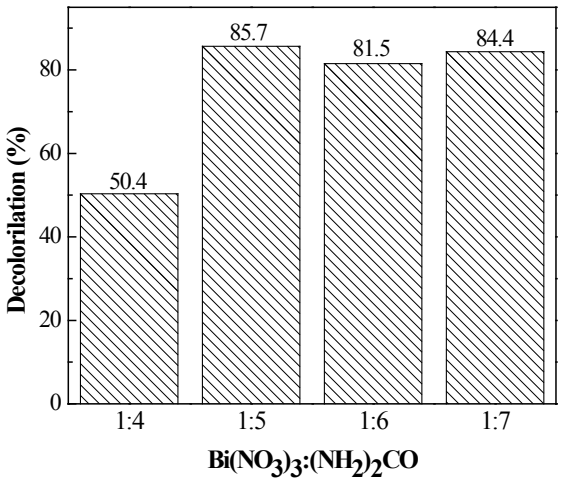

Fig. 7. Photocatalytic activity of the photocatalysts.

demonstrating that the relative high photocatalytic activity of the1:5 sample is mainly assigned to its higher photo-generated carriers separation efficiency as compared to other samples.

3.2. Photocatalytic activity

The photocatalytic activities of the as-prepared samples were evaluated by the degradation of MO. Without the presence of photocatalyst, the photolysis of MO can be totally ignored. The dark absorption of MO over the different photocatalysts after 40 min is less than 7%. Fig. 7 depicts the photocatalytic activity of the as-prepared samples. It is clear that only 50.35% MO was decomposed over the 1:4 sample under the simulated solar light irradiation for 40 min, whereas the 1:5, 1:6 and 1:7 samples display much higher photocatalytic activities with more than 80% MO was degraded in the same period of time, and the 1:5 sample exhibits the best photocatalytic performance with 85.66% MO degradation efficiency, indicating that 1:5 is the optimal Bi/C molar ratio for $(BiO)_2CO_3$ synthesis. Moreover, it is interesting to note that when the molar ratio of Bi/C ≦ 1/5, the differences between the photocatalytic activities of the different samples are less significant, the detailed mechanism still remains to be further explored. Based on all the results discussed, photo-generated carriers separation efficiency is the decisive factor, resulting in the diverse photocatalytic activities of $(BiO)_2CO_3$ prepared with different reactants molar ratio in this work.

4. Conclusions

In summary, the influence of different reactants ratios on the photocatalytic activity of $(BiO)_2CO_3$ prepared by a facile hydrothermal method using bismuth nitrate pentahydrate ($Bi(NO_3)_3{\cdot}5H_2O$) and urea with different molar ratios was successfully investigated. The results manifest that different molar ratios of Bi/C play a critical role in determining the photocatalytic performance of $(BiO)_2CO_3$. The highest degradation efficiency of MO by as-prepared $(BiO)_2CO_3$ photocatalysts can reach 85.66% under the simulated solar light irradiation for 40 min when the molar ratio of Bi/C is 1/5. The superior photocatalytic activity of the 1:5 sample can be definitely attributed to its highest photo-generated carriers separation rate in this work.

Acknowledgements

This project was financially supported by the Opening Project of Jiangsu Key Laboratory for Environment Functional Materials (No. SJHG1307).

References

[1] H.W. Tian, M. Liu, W.T. Zheng, Constructing 2D graphitic carbon nitride nanosheets/layered MoS_2/graphene ternary nanojunction with enhanced photocatalytic activity, Appl. Catal. B: Environ., 225 (2018) 468–476.
[2] Y.T. Xiao, G.H. Tian, Y.J. Chen, X. Zhang, H.Y. Fu, H.G. Fu, Exceptional visible-light photoelectro catalytic activity of In_2O_3/In_2S_3/CdS ternary stereoscopic porous heterostructure film for the degradation of persistent 4-fluoro-3-methylphenol, Appl. Catal. B: Environ., 225 (2018) 477–486.
[3] V. Vaianoa, M. Matarangolo, J.J. Murcia, H. Rojas, J.A. Navío, M.C. Hidalgo, Enhanced photocatalytic removal of phenol from aqueous solutions using ZnO modified with Ag, Appl. Catal. B: Environ., 225 (2018) 197–206.
[4] Z. Song, X.L. Dong, N. Wang, L.H. Zhu, Z.H. Luo, J.D. Fang, C.H. Xiong, Efficient photocatalytic defluorination of perfluorooctanoic acid over BiOCl nanosheets via a hole direct oxidation mechanism, Chem. Eng. J., 317 (2017) 925–934.
[5] M. Sansotera, F. Persico, C. Pirola, W. Navarrini, A.D. Michele, C.L. Bianchia, Decomposition of perfluorooctanoic acid photocatalyzed by titanium dioxide: Chemical modification of the catalyst surface induced by fluoride ions, Appl. Catal. B: Environ., 148–149 (2014) 29–35.
[6] J. Zhong, J. Li, S. Huang, C. Cheng, W. Yuan, M. Li, J. Ding, Improved solar-driven photocatalytic performance of Ag_2CO_3/$(BiO)_2CO_3$ prepared in-situ, Mater. Res. Bull., 77 (2016) 185–189.
[7] J. Chen, J. Zhong, J. Li, S. Huang, Z. Xiang, M. Li, Effects of the molar ratio on the photo-generated charge separation behaviors and photocatalytic activities of $(BiO)_2CO_3$-BiOBr composites, Solid State Sci., 60 (2016) 11–16.

[8] Y. Si, J. Li, J. Zhong, J. Zeng, S. Huang, W. Yuan, M. Li, J. Ding, Charge separation properties of $(BiO)_2CO_3$/BiOI heterostructures with enhanced solar-driven photocatalytic activity, Curr. Appl. Phys., 16 (2016) 240–244.
[9] Q. Yang, J. Li, J. Zhong, C. Cheng, Z. Xiang, J. Chen, Enhanced solar photocatalytic performance of $(BiO)_2CO_3$ prepared with the assistance of ionic liquid, Mater. Lett., 192 (2017) 157–160.
[10] Y. Zheng, F. Duan, M.Q. Chen, Y. Xie, Synthetic $Bi_2O_2CO_3$ nanostructures: novel photocatalyst with controlled special surface exposed, J. Mol. Catal. A: Chem., 317 (2010) 34–40.
[11] H.W. Huang, Y. He, Z.S. Lin, L. Kang, Y.H. Zhang, Two novel Bi-based borate photocatalysts: crystal structure, electronic structure, photoelectro chemical properties, and photocatalytic activity under simulated solar light irradiation, J. Phys. Chem. C., 117 (2013) 22986–22994.
[12] H.W. Huang, X.W. Li, J.J. Wang, F. Dong, P.K. Chu, T.R. Zhang, Y.H. Zhang, Anionic group self-doping as a promising strategy: band-gap engineering and multi-functional applications of high-performance CO_3^{2-} doped $Bi_2O_2CO_3$, ACS Catal., 5 (2015) 4094–4103.
[13] T. Xiong, X.A. Dong, H.W. Huang, W.L. Cen, Y.X. Zhang, F. Dong, Single precursor mediated-synthesis of Bi semimetal deposited N-doped $(BiO)_2CO_3$ superstructures for highly promoted photcatalysis, ACS Sustain. Chem. Eng., 4 (2016) 2969–2979.
[14] X.F. Cao, L. Zhang, X.T. Chen, Z.L. Xue, Persimmon-like $(BiO)_2CO_3$ microstructures: hydrothermal preparation, photocatalytic properties and their conversion into Bi_2S_3, Cryst. Eng. Comm., 13 (2011) 1939–1945.
[15] F. Dong, P.D. Li, J.B. Zhong, X.Y. Liu, Y.X. Zhang, W.L. Cen, H.W. Huang, Simultaneous Pd^{2+} doping and Pd metal deposition on $(BiO)_2CO_3$ microspheres for enhanced and stable visible light photocatalysis, Appl. Catal., A 510 (2016) 161–170.
[16] X. Dong, W. Zhang, W. Cui, Y. Sun, H. Huang, Z. Wu, F. Dong, Pt quantum dots deposited on N-doped $(BiO)_2CO_3$: enhanced visible light photocatalytic NO removal and reaction pathway, Catal. Sci. Technol., 7 (2017) 1324–1332.
[17] T. Xiong, M.Q. Wen, F. Dong, J.Y. Yu, L.L. Han, B. Lei, Y.X. Zhang, X.S. Tang, Z.G. Zang, Three dimensional Z-scheme $(BiO)_2CO_3/MoS_2$ with enhanced visible light photcatalytic NO removal, Appl. Catal. B: Environ., 199 (2016) 87–95.
[18] T.Y. Zhao, J.T. Zai, M. Zou, Q. Zou, Y.Z. Su, K.X. Wang, X.F. Qian, Hierarchical $Bi_2O_2CO_3$ microspheres with improved visible-light-driven photocatalytic activity, Cryst. Eng. Comm., 13 (2011) 4010–4017.
[19] X. Feng, W. Zhang, Y. Sun, H. Huang, F. Dong, Fe(III) clusters-grafted $(BiO)_2CO_3$ superstructures: In situ DRIFTS investigation on IFCT-enhanced visible light photocatalytic NO oxidation, Environ. Sci. Nano, 4 (2017) 604–612.
[20] X. Feng, W. Zhang, H. Deng, Z. Ni, F. Dong, Y. Zhang, Efficient visible light photocatalytic NOx removal with cationic Agclusters-grafted $(BiO)_2CO_3$ hierarchical superstructures, J. Hazard. Mater., 322 (2017) 223–232.
[21] P.M. Schaber, J. Colson, S. Higgins, D. Thielen, B. Anspach, J. Brauer, Thermal decomposition (pyrolysis) of urea in an open reaction vessel, Thermochimica Acta, 424 (2004) 131–142.
[22] J. Zhong, J. Li, F. Feng, Y. Lu, J. Zeng, W. Hu, Z. Tang, Improved photocatalytic performance of SiO_2-TiO_2 prepared with the assistance of SDBS, J. Mol. Catal. A: Chem., 357 (2012) 101–105.
[23] L.Q. Ye, J.Y. Liu, Z. Jiang, T.Y. Peng, L. Zan, Facets coupling of BiOBr-g-C_3N_4 composite photocatalyst for enhanced visible-light-driven photocatalytic activity, Appl. Catal. B: Environ., 142–143 (2013) 1–7.
[24] A.R. Gandhe, J.B. Fernandes, A simple method to synthesize N-doped rutile titania with enhanced photocatalytic activity in sunlight, J. Solid State Chem., 178 (2005) 2953–2957.
[25] J. Cao, X. Li, H.L. Lin, S.F. Chen, X.L. Fu, In situ preparation of novel *p-n* junction photocatalyst BiOI/$(BiO)_2CO_3$ with enhanced visible light photocatalytic activity, J. Hazard. Mater., 239–240 (2012) 316–324.
[26] P. Madhusudan, J.R. Ran, J. Zhang, J.G. Yu, G. Liu, Novel urea assisted hydrothermal synthesis of hierarchical $BiVO_4$/$Bi_2O_2CO_3$ nanocomposites with enhanced visible-light photocatalytic activity, Appl. Catal. B: Environ., 110 (2011) 286–295.
[27] L. Kronik, Y. Shapira, Surface photovoltage phenomena: theory, experiment and application, Surf. Sci. Rep., 254 (1999) 1–205.
[28] L.S. Zhang, K.H. Wong, H.Y. Yip, C. Hu, J.C. Yu, C.Y. Chan, P.K. Wong, Effective photocatalytic disinfection of e. coli K-12 using AgBr-Ag-Bi_2WO_6 nanojunction system irradiated by visible light: the role of diffusing hydroxyl radicals, Environ. Sci. Technol., 44 (2010) 1392–1398.
[29] Y.X. Chen, S.Y. Yang, K. Wang, L.P. Lou, Role of primary active species and TiO_2 surface characteristic in UV-illuminated photodegradation of acid orange 7, J. Photochem. Photobiol. A: Chem., 172 (2005) 47–54.
[30] N. Zhang, S.Q. Liu, X.Z. Fu, Y.J. Xu, Synthesis of M@TiO_2 (M = Au, Pd, Pt) core-shell nanocomposites with tunable photoreactivity, J. Phys. Chem. C., 115 (2011) 9136–9145.
[31] M.C. Yin, Z.S. Li, J.H. Kou, Z.G. Zou, Mechanism investigation of visible light-induced degradation in a heterogeneous TiO_2/eosin Y/rhodamine B system, Environ. Sci. Technol., 43 (2009) 8361–8366.
[32] X. Xu, X. Duan, Z. Yi, Z. Zhou, X. Fan, Y. Wang, Photocatalytic production of super oxide ion in the aqueous suspensions of two kinds of ZnO under simulated solar light, Catal. Commun., 12 (2010) 169–172.